KSME

Springer

Journal of Mechanical Science and Technology 38 (8) 2024

Original Article
DOI 10.1007/s12206-024-0711-y

Keywords:
· Al/Mg
· ANOVA
· Behaviour studies
· Microstructure
· Machining studies

Correspondence to:
R. Venkatesh
venkatindustrial@gmail.com

Citation:
Venkatesh, R., Logesh, K., Singh, S., Singh, P. K., Hossain, I., Mohanavel, V., Soudagar, M. E. M., Alharbi, S. A., Obaid, S. A. (2024). Aluminium alloy nanocomposite made with SiC via ultrasonic stir casting: Behaviour study. Journal of Mechanical Science and Technology 38 (8) (2024) 4145~4151.
http://doi.org/10.1007/s12206-024-0711-y

Received February 7th, 2024
Revised April 25th, 2024
Accepted April 26th, 2024

† Recommended by Editor
Jun-Hyub Park

Aluminium alloy nanocomposite made with SiC via ultrasonic stir casting: Behaviour study

R. Venkatesh[1], K. Logesh[2], Satyendra Singh[3], Pradeep Kumar Singh[4], Ismail Hossain[5], V. Mohanavel[6,7], Manzoore Elahi M. Soudagar[8,9], Sulaiman Ali Alharbi[10] and Sami Al Obaid[11]

[1]Department of Mechanical Engineering, Saveetha School of Engineering, Saveetha Institute of Medical and Technical Sciences, (SIMATS), Saveetha University, Chennai 602105, Tamilnadu, India, [2]Department of Mechanical Engineering, Vel Tech Rangarajan Dr.Sagunthala R&D Institute of Science and Technology, Chennai, Tamil Nadu, India, [3]Chitkara Centre for Research and Development, Chitkara University, Himachal Pradesh 174103, India, [4]Department of Mechanical Engineering, Institute of Engineering & Technology, GLA University, Mathura, Uttar Pradesh 281001, India, [5]Department of Nuclear and Renewable Energy, Ural Federal University, Yekaterinburg 620002, Russia, [6]Centre for Materials Engineering and Regenerative Medicine, Bharath Institute of Higher Education and Research, Chennai 600073, Tamil Nadu, India, [7]Department of Mechanical Engineering, Amity University, Dubai 345019, United Arab Emirates, [8]Department of Mechanical Engineering, Graphic Era (Deemed to be University), Dehradun, Uttarakhand 248002, India, [9]Department of Mechanical Engineering, Chandigarh University, Mohali 140413, Punjab, India, [10]Department of Botany and Microbiology, College of Science, King Saud University, PO Box -2455, Riyadh -11451, Saudi Arabia, [11]Department of Botany and Microbiology, College of Science, King Saud University, PO Box -2455, Riyadh -11451, Saudi Arabia

Abstract The research attempted to enrich the aluminium alloy (Al/Mg) nanocomposite with silicon carbide (SiC). The ultrasonic assist stir cast established that the Al/Mgnanocomposite is involved in microstructure, hardness and tensile performance. Its result is uniform dispersion without agglomeration, and 7.5 wt% SiC owns higher microhardness and better tensile strength of 161±1.5 H V and 238±2 MPa. This nano Al/Mg alloy composite is subjected to machining studies by using a vertical CNC milling setup & titanium nitride (TiN) coated end mill functioned by 300-1200 rpm spindle speed (N), 0.01-0.04mm/rev feed rate (FR) and 0.1-0.4 mm depth of cut (DOC). The impact DOC, FR, and N on material removal rate (MRR), temperature (T), and tool wear (Tw) are measured, and the L16 design experiment (ANOVA-GLM) is defined. Finally, the best interaction input milling parameter pairs on obtaining high MRR with the least T and Tw. The DOC is the most significant factor in controlling the MRR, T and Tw.

1. Introduction

Composite is the trend for high strength-to-weight ratio applications, and hybrid Al/Mg composites have the potential for technical applications [1], referred to as liquid processing [2]. Conventional liquid processing exposed casting defects, which are overcome by the advanced vacuum die-cast process [3]. The A356/1-5 % SiC is made via stir cast, and studied its microstructure and mechanical behaviour. Deep dispersion of SiC in A356 alloy is spotted via microstructure analysis. It results in improved mechanical behaviour of composites [4]. Hybrid nano Al/Mg composite mechanical behaviour was enriched by the incorporation of multi-ceramic reinforcements and attained homogenous particle distribution due to constant stir speed [5] and ultrasonic-assisted stir cast process [6]. Besides, the liquid stir cast found significant choices in complex shape fabrication and cost-effective routes rather than others [7]. However, the SiC-incorporated aluminium alloy composite has excellent mechanical characteristics [8]. During the machinability studies of composites, high tool wear, increased frictional temperature, and poor surface quality are spotted by uncoated tools [9, 10]. Using a titanium nitride (TiN) end mill during the machining of aluminium composite for aerospace applications found good tool life

and increased surface quality [11]. The N, FR, and axial depth effect on end milling operation aluminium alloy temperature were studied with high-speed steel. Its parameters were optimized through the ANOVA technique [12]. The ANOVA grey relation analysis with the L27 design run was utilized to optimize the BT40 end mill tool holder operated end milling parameters like N, FR, and DOC on least surface roughness, higher MRR, and low cutting force identified [13]. Aluminum titanium nitride (TiAlN) coated end milling tool used for aluminium alloy nanocomposite machining under different milling parameters and measuring the surface integrity. The TiAlN-coated tool performed composite found a good surface finish after the end milling process [14]. The CNC end milling operation of AA3105 aluminium alloy was machined with various input machining parameters, and its parameters were optimized via a multi-response technique found low surface roughness of 0.4651 μm under the parameters of 1.54 mm tool depth, 1646 rpm spindle speed, and 4.66 m/sec feed rate [15]. The aluminium alloy AA6082-T6 was machined by dry state end milling process with different levels of N, FR, and DOC by using the ANOVA approach, and the input desirability was optimized and obtaining the high machining quality and larger MRR, and economic [16]. Optimum machining parameters for the face milling operation of metal matrix composite were optimized through grey relational analysis. Its results showed the optimum milling parameters for reaching the larger MRR and least tool wear. The Mg/B_4C composite is involved in to end milling process and studies its surface quality via Talysuf meter [17].

Moreover, the high speed milling process found better surface quality [18], and the coated end mill found lower tool wear than conventional [19]. The novel research seeks to enrich the composite's behaviour by incorporating nano SiC particles through ultrasonic-assisted stir cast technology. The effect of SiC on microstructure, hardness, and tensile performance of Al/Mg composite is studied, and the nanocomposite consisting of 7.5 wt% SiC has better results and involves machining studies. The optimum machining process parameters were noted by ANOVA analysis. The output response, such as higher MRR, lower temperature, and lower tool wear, was noted to have significant input factors in their levels.

2. Methods

2.1 Processing of composites

According to Table 1, the Al/Mg alloy nanocomposite is processed with nano SiC particles via an ultrasonic adopted stir cast process. Before this, 90 % aluminium and 10 % magnesium with 99.9 % purity were chosen as base metals due to their lightweight, enhanced tensile strength, good castability and better thermal stability. With the qualities of better thermal stability, higher hardness, high modulus of rigidity, and high melting point [5] reasons, the 50 nm SiC particles are considered the reinforcement phase.

Table 1. Compositions of matrix and SiC.

Materials/samples	Al/Mg	N1	N2	N3
Al/Mg	100	97.5	95	92.5
SiC	0	2.5	5	7.5

Using a graphite-made crucible, the Al/Mg metal pieces are loaded and heated at 350 °C and melted at 700 °C under an argon atmosphere limiting the oxidation g1]. In the meantime, the nano Sic. particles were heated externally at 300 °C for the durations of 10 mis supports to eliminate the moisture [3, 4]. Then, it is dropped into molten slurry and mixed via an ultrasonic-assisted stirrer with an applied speed of 500 rpm for 10 minutes. Afterwards, the blended molten metal is accessed with a bottom pouring setup, and the casting uses a tool steel die with dimensions of 250 mm×100 mm×15 mm, respectively. Finally, the composite behaviour of hardness and tensile is studied by ASTM E-384 and E8 standards [1]. The composite sample was taken with the dimension of 100 mm×100 mm× 10 mm, which was suitable for the end milling process via XL MILL model CNC end mill [7]. The 10 mm TiN-coated end mill tool was used for this study due to its enhanced hardness of 2400 Hv, reduced friction, higher chip flow and superior lubricity [11].

2.2 End milling operation

The XL MILL type portable bench milling machine is configured with CNC Fanuc control, which consists of a taper spindle model R8, an automatic tool changer (ATC) model of BT35 and a table with three TEE slots that provide sufficient holding of the workpiece. With the help of the table, the aluminium alloy hybrid nanocomposite was placed, and the TiN tool was kept in ATC. Throughout the end, the milling operation was made with the TiN tool. To find the material removal rate, the composite material was weighed before and after a digital stopwatch recorded the end of the milling operation and the machining time. The milling tool dynamometer monitored the cutting force and tool wear during the end milling operation. Three stages noted the temperature of the end milling machining process: starting, half of depth machine, and end of machining. The average of three is considered as mean temperature.

2.3 ANOVA design details with GLM

In the current study, the speed (N), feed rate (f), and depth of cut (DOC) are treated as input factors, and their values are varied by 300-1200 rpm speed, 0.01-0.04 mm/rev feed rate and 0.1-0.4 mm depth of cut are treated as levels. The parameters are chosen with the references of past Refs. [11, 16]. Concerning the input factor being 3 and its levels being 4, the design analysis was selected by the option for the number of factors 3, and the design level was 4. The design details of Taguchi are shown in Table 2.

The optimum experiment design was selected as L16; its de-

Table 2. Taguchi design.

N	rpm	300	600	900	1200
F	rev/min	0.01	0.02	0.03	0.04
DOC	mm	0.1	0.2	0.3	0.4

Table 3. Design sequence – L16 (run R1-R16).

Design sequence	N	f	DOC	t	MRR	Tavg	Tw
	rpm	mm/rev	mm	sec	g/sec	°C	µm
L1	300	0.01	0.1	98	0.011	91.73	0.39
L2		0.02	0.2	101	0.012	89.5	0.29
L3		0.03	0.3	106	0.012	89.23	0.19
L4		0.04	0.4	110	0.015	93.83	0.17
L5	600	0.01	0.2	100	0.014	92.17	0.39
L6		0.02	0.1	95	0.012	92.53	0.48
L7		0.03	0.4	108	0.017	92.23	0.21
L8		0.04	0.3	107	0.015	94.97	0.19
L9	900	0.01	0.3	106	0.017	91.8	0.23
L10		0.02	0.4	111	0.018	97.83	0.2
L11		0.03	0.1	97	0.01	96.57	0.39
L12		0.04	0.2	102	0.014	94.2	0.29
L13	1200	0.01	0.4	112	0.019	102.8	0.2
L14		0.02	0.3	107	0.017	99.77	0.21
L15		0.03	0.2	104	0.015	92.73	0.29
L16		0.04	0.1	100	0.011	100.3	0.41

tails are shown in Table 3. The main effects plot for the mean value of input factors with related output response shows their rank order. Next level, the GLM was executed with 99.5 % confidence level.

3. Results and discussions

3.1 Morphology studies

For easy-to-understand particle distribution and structure formation, the microstructure of the ultrasonic adopted stir cast samples is presented in Figs. 1(a)-(d) with 5000x magnification. The structure is illustrated here based on the Al/Mg merged with nano SiC particles. Fig. 1(a) indicates the Al/Mg alloy casted sample microstructure and the Mg inter-metallic phase. There were no identical casting defects, and the structure showed that dendrite-linked coarse structure supports good thermal stability. Besides, the dendrite structure is formed due to high solidification temperature. Likewise, previous literature found similar grains while evaluating Al/Mg alloy cast [5]. Fig. 1(b) displays the morphology of the N1 composite sample prepared with 2.5 wt% of nano SiC particles, showing the black dotted field along the Al/Mg matrix. The dendrite structure indicates the Al/Mg interface. Besides, the constant stir speed with ultrasonic assistance may lead to wide dispersion of nano SiC particles. A few SiC particles merged due to unavoidable

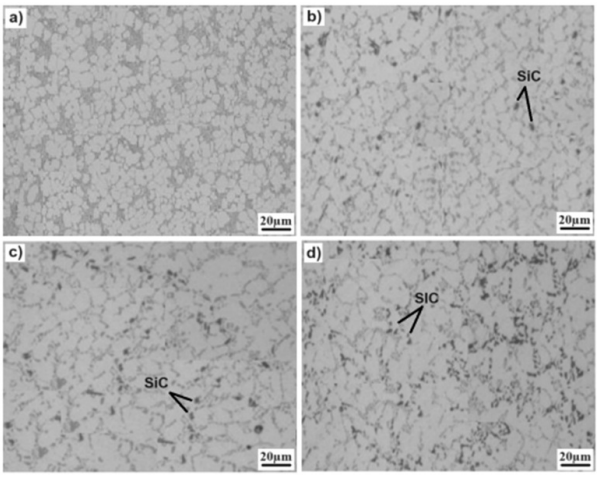

Fig. 1. Surface morphology of (a) Al/Mg; (b) N1; (c) N2; (d) N3 sample.

blending actions [4]. However, the nano SiC particles were identified in the Al/Mg matrix. The morphology of N2 and N3 composite samples established with 5 wt% and 7.5 wt% of nano SiC particles via ultrasonic assist stir cast technique is displayed in Figs. 1(c) and (d). Fig. 1(c) shows the uneven particle distribution with a reduced particle gap. Most SiC particles were merged with adjusting SiC particles due to unrated solidification stir temperature [3]. However, no casting defects were recorded in the morphology image. Likewise, Fig. 1(d) shows the morphology of the N3 composite sample made with a higher content of SiC particles and distributed homogenously in the Al/Mg matrix. The coarse grains of SiC particles make the perfect bonding with the Al/Mg alloy matrix, resulting in better stability and enduring the maximum load during the mechanical evaluations of the composite sample.

3.2 Microhardness performance

Conventional aluminium has a moderate microhardness value, and the present investigation aims to enrich the aluminium microhardness value by introducing nano SiC particles. Fig. 2 depicts the microhardness of the aluminium alloy casted sample (Al/Mg) and nano SiC incorporated Al/Mg alloy nanocomposite with a permissible error value of 5 %. The experimental average Al/Mg alloy casted sample microhardness value is 125±1 HV. This value matches nearer the earlier reported value [1]. Besides, identifying nano SiC as 2.5 wt% in the Al/Mg alloy matrix liberates 142±2 HV. This value exceeds the Al/Mg caste sample's hardness value. The appearance of nano SiC particles with coarse grain causes a better hardness value [3, 4].

Even as 5 wt% and 7.5 wt% of nano SiC contribute with Al/Mg matrix offered excellent microhardness value due to efficient pinning action between matrix and SiC, as evidenced in Figs. 1(c) and (d). The microhardness of the N2 composite sample with 5 wt% nano SiC showed 154±2 HV and hiked by 161±2 HV on the inclusions of 7.5 wt% of nano SiC. The SiC

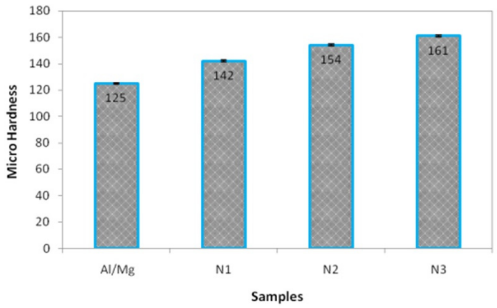

Fig. 2. Microhardness of composite samples.

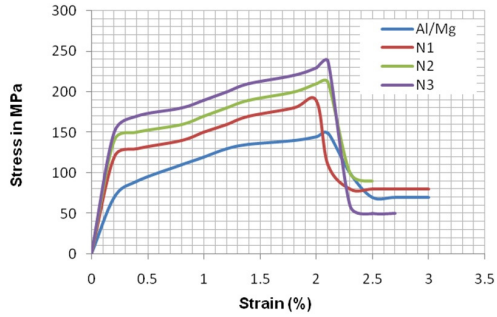

Fig. 3. Stress-strain deformation curve.

made with Al/Mg as perfect bonding results improved the hardness of the composite [5]. However, the N3 nanocomposite sample consists of 7.5 wt% of nano SiC proved and attained 29 % improvement on related with Al/Mg casted sample.

3.3 Tensile stress behaviour

The 90 % Al and 10 % Mg combinations adopted with nano SiC particles facilitate good tensile stress performance rather than monolithic Al and Mg materials. The purpose of showing the research results for Al/Mg alloy and its nanocomposite tensile stress is illustrated in Fig. 3 with an allowable error value of 5 %. The Al/Mg casted sample's tensile stress value is 149±2 MPa, which is higher than the tensile strength of pure Al metal [2]. Even the adaptations of nano SiC particles in the Al/Mg matrix show uptrend movement in tensile stress and are higher than the Al/Mg cast value. The appearance of nano SiC with homogenous particle dispersion is the reason for improved tensile stress.

Moreover, the N1 composite sample adopted with 2.5 wt% of nano SiC is noted by 187±3 MPa. Likewise, the N2 composite sample of 5 wt% nano SiC indicates the hiked tensile stress value of 212±3 MPa because effective intermixed matrix and nano SiC could endure the maximum load. The same approach was reported while evaluating Al/Mg alloy composite [5]. Besides, the N3 composite sample (Al/Mg/7.5 wt %) recorded maximum tensile stress (238±2 MPa), 59.7 % greater than the casted Al/Mg alloy sample. Compared to past reported value [1], it was enriched by 2 %.

However, the higher loading of SiC attained better tensile stress value than other composite samples. The process parameters and operating conditions (ultrasonic stirrer & preheating effect of the mould die) were the specific reasons for the improved mechanical performance of the composite [7]. Moreover, the hardness and tensile strength behaviour is addressed in detail.

Table 4. Analysis of variance for MRR, using adjusted SS for tests.

Source	DF	Seq SS	Adj SS	Adj MS	F	P	Rank
DOC	3	8.32E-05	8.32E-05	2.77E-05	38.03	0	1
N	3	1.97E-05	1.97E-05	6.60E-06	9	0.012	2
f	3	8.20E-06	8.20E-06	2.70E-06	3.74	0.079	3
Error	6	4.40E-06	4.40E-06	7.00E-07			-
Total	15	1.15E-04					-

S = 0.000853913 R-Sq = 96.21 % R-Sq(adj) = 90.53 %

3.4 Details for metal removal rate (MRR) – larger is better

The metal removal rate mainly depends on the depth of the cut [13]. The design analysis is executed with N, f, and DOC under the option for larger output, which is better. The main effect plot mean value for optimum end milling MRR is fixed as 0.01475 g/sec, and the analysis showed the 0.3-0.4 mm depth of cut, 600-1200 rpm speed, and 0.01-0.02 mm/rev is the best parameters for obtaining higher MRR. In a past report, the DOC and feed rate were significant factors for increased MRR [15].

Based on this design, the GLM approach was implemented with 99.5 % confidence. Its F-test proved the significance of the end milling parameter contribution rate with its percentage shown in Table 4. It is noted from Table 4 that the DOC is performed at a higher level with a contribution of 72.10 %. While compared to other factors, it plays an important role in deciding the MRR. The generated values meet 96.21 % R-sq value, which results in good TiN coated end mill performance during Al/Mg alloy hybrid nanocomposite.

With the help of GLM, the residual plots for MRR are illustrated in Fig. 4. The best sequences predicted from Fig. 4 related to design analysis are L7-L8-L9-L10-L13- and L-14.

3.5 Details for temperature (T_{avg}) - smaller is better

Temperature during the machining process increased due to the high friction between the tool and workpiece [10]. The present investigation used TiN coated end mill tool and found good thermal stability during the high-speed machining process [11].

In the design approach, the temperature-controlling input factors with their levels are predicted by the smaller option, which is better. The results showed the rank order as 1, 2, and 3, N, DOC, and f, respectively, shown in Table 5.

Table 5. Analysis of variance for T_{avg}, using adjusted SS for tests.

Source	DF	Seq SS	Adj SS	Adj MS	F	P	Rank
N	3	135.171	135.171	45.057	8.7	0.013	1
DOC	3	44.659	44.659	14.886	2.9	0.126	2
f	3	20.851	20.851	6.95	1.3	0.346	3
Error	6	31.084	31.084	5.181			-
Total	15	231.766					-

S = 2.27610 R-Sq = 86.59 % R-Sq(adj) = 66.47 %

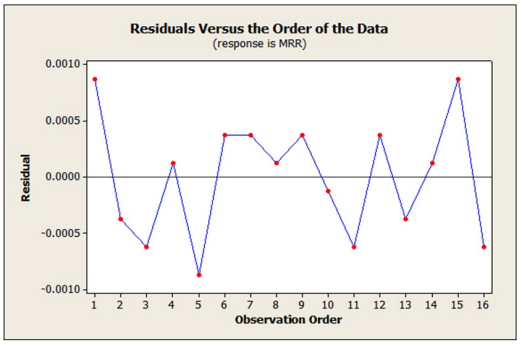

Fig. 4. Residuals versus design of experiment MRR data.

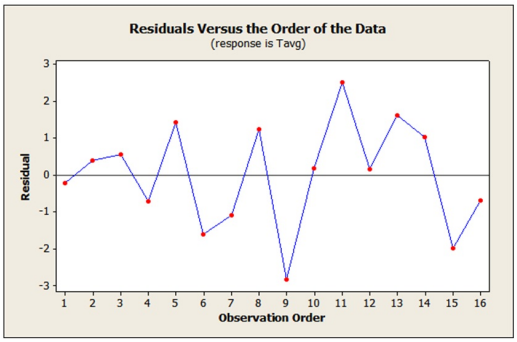

Fig. 5. Residuals versus design of experiment temperature (T_{avg}) data.

Concerning the ANOVA, GLM was executed at a 99.5 % confidence level. The results of the analysis of variance for Tavg, using adjusted SS for tests (F-test), showed their contribution of input factors like N-58.32 %, DOC-19.27 %, and f-9 % under the R-sq of 86.59 %. So, the temperature control input end mill parameters are N and DOC. There was no major effect during the variation of feed rate.

The optimum combination predicted from the design mean is 300-600 rpm speed, 0.2-0.3 depth of cut, and 0.01, 0.02, and 0.03 mm/rev. Finally, the GLM predicted residual plot for temperature variation among the L16 experiments is shown in Fig. 5. It illustrates the graph between the residuals versus the experiment design on temperature data. This plot was related to the design's main effect plot mean value for temperature, which is L2-L3-L5-and L8.

3.6 Details for tool wear (T_w) - smaller is better

Table 6. Analysis of variance for T_w, using adjusted SS for tests.

Source	DF	Seq SS	Adj SS	Adj MS	F	P	Rank
DOC	3	0.131769	0.131769	0.043923	70	0	1
N	3	0.007119	0.007119	0.002373	3.8	0.079	2
f	3	0.004069	0.004069	0.001356	2.2	0.195	3
Error	6	0.003787	0.003787	0.000631			-
Total	15	0.146744					-

S = 0.0251247 R-Sq = 97.42 % R-Sq(adj) = 93.55 %

Table 7. Optimum machining parameters for higher MRR, low temperature and low tool wear.

Design sequences	N	f	DOC	t	MRR	T_{avg}	T_w
	rpm	mm/rev	mm	Sec	g/sec	°C	µm
L8	600	0.04	0.3	107	0.015	94.97	0.19

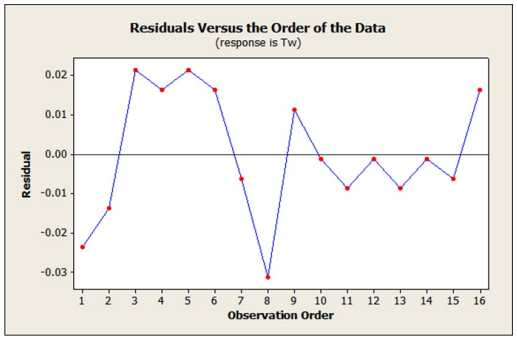

Fig. 6. Residuals versus tool wear (T_w).

The experimental results on tool wear are found to be minimal, and their details are summarized in Table 3. Compared to conventional tools, the coated tool found less wear rate, increased tool life and good surface finish [11, 14]. The design approach is executed with the response of tool wear controlling the input factor model, which is defined by smaller being better. The main effect plot for tool wear means found by 0.2775 µm. With this reference value, the following DOC (0.3-0.4 mm), N (300-1200 rpm), and f (0.01-0.04 mm/rev) factors and levels are found as best combinations for lower tool wear, which is less than the mean value. The 99.5 % confidence level GLM executed results of analysis of variance for T_w, using adjusted SS for tests (F-test), is mentioned in Table 6. It found DOC contributes 89.80 % to deciding the tool wear. The speed and feed rate showed very little contribution and were related to DOC, and it was less than 5 %.

Fig. 6 indicates the scatter plot for the residual value for tool wear generated by the GLM approach with the L16 experiment design. The possible interaction factors with their levels are related to the main effect plot for tool wear mean value, and we found L3-L4-L7-L8-L9-and L10 to be the best interaction to achieve the least tool wear.

The best interaction design sequence for obtaining higher MRR, least temperature, and low tool wear are compared. The

similar design sequence, which meets all three responses, is found as L8, and its details are mentioned below in Table 7.

4. Conclusions

With the support of an ultrasonic stirrer, the Al/Mg alloy and its nanocomposites are developed with 2.5, 5, and 7.5 wt% of nano SiC particle via stir casting route and their structural morphology, hardness, and tensile stress behaviour are investigated by ASTM standard. The morphology studies revealed that the nano SiC particles are spread over the Al/Mg matrix as homogenous, and the N3 composite (Al/Mg/7.5 wt% SiC) own excellent hardness and tensile stress value, which is hiked by 29 % and 59.7 % comparably Al/Mg alloy cast hardness and tensile stress value. This N3 composite is involved in machining studies. The TiN-coated end mill tool used dry milling operation for Al/Mg/7.5 wt% of nano SiC, machined by different factors and levels. The output MRR, temperature, and tool wear are measured, and the effect of input end milling factors on output response was optimized via the ANOVA Taguchi GLM technique with a 99.5 % confidence level. The successful design analysis was executed with the L16 design of the experiment, and output response control factors with their levels were found using the main effect plot and residuals plot. Each response control input factor was summarized, and the L8 design sequence found the best interaction, which offered a larger MRR (0.015 g/cc) at least frictional temperature (94.97 °C), resulting in low tool wear (0.19 µm).

Acknowledgements

This project was supported by Researchers Supporting Project number (RSP2024R315) King Saud University, Riyadh, Saudi Arabia. The research funding from the Ministry of Science and Higher Education of the Russian Federation (Ural Federal University Program of Development within the Priority-2030 Program) is gratefully acknowledged.

References

[1] K. R. Padmavathi et al., Synthesis of Al/Mg hybrid nanocomposite by electromagnetic stir cast: characteristics study, *Silicon*, 15 (2023) 7383-7392.

[2] A. Sankhala and K. M. Patel, Metal matrix composites fabricated by stir casting process–a review, *Advances in Materials and Processing Technologies*, 8 (2) (2021) 1270-1291.

[3] A. Baraniraj et al., Vacuum stir cast developed aluminium alloy hybrid nanocomposite performance compared with gravity cast: mechanical and tribological characteristics study, *International Journal of Metalcasting*, 18 (2023) 1273-1283.

[4] M. T. Alam et al., Mechanical properties and morphology of aluminium metal matrix nanocomposites-stir cast products, *Advances in Materials and Processing Technologies*, 3 (4) (2017) 600-615.

[5] P. R. Sekaran et al., Mechanical and physical characterization studies of nano ceramic reinforced Al-Mg hybrid nanocomposites, *Silicon*, 15 (2023) 4555-4567.

[6] P. Madhukar et al., Fabrication and characterization two step stir casting with ultrasonic assisted novel AA7150-hBN nanocomposites, *Journal of Alloys and Compounds*, 815 (2020) 152464.

[7] M. S. Kadam and V. D. Shinde, Stir cast aluminium metal matrix composites with mechanical and micro-structural behaviour: a review, *Materials Today Proceedings*, 27 (2) (2020) 845-852.

[8] N. J. Abdulkader and M. S. Abed, Influence of SiC nanoparticles addition on the microstructure and mechanical properties of stir-casted Zn-Al alloy, *International Journal of Cast Metals Research*, 36 (4) (2023) 142-150.

[9] A. F. V. Pedroso et al., A comprehensive review on the conventional and non-conventional machining and tool-wear mechanisms of INCONEL, *Metals*, 13 (3) (2023) 585.

[10] M. K. Gupta et al., Comparison of tool wear, surface morphology, specific cutting energy and cutting temperature in machining of titanium alloys under hybrid and green cooling strategies, *International Journal of Precision Engineering and Manufacturing-Green Technology*, 10 (2023) 1393-1406.

[11] R. S. Kumar et al., Optimization of high speed CNC end milling process of bsl 168 aluminium composite for aeronautical applications, *Transactions of the Canadian Society for Mechanical Engineering*, 41 (4) (2018) 609-625.

[12] V. S. Kaushik et al., Optimization of processes parameters on temperature rise in CNC end milling of al 7068 using hybrid techniques, *Materials Today Proceedings*, 5 (2) (2018) 7037-7046.

[13] M. B. Kumar et al., Parameters optimization for end milling of Al7075-ZrO_2-C metal matrix composites using GRA and ANOVA, *Transactions of the Indian Institute of Metals*, 73 (2020) 2931-2946.

[14] N. S. K. Reddy et al., Experimental study of surface integrity during end milling of Al/SiC particulate metal–matrix composites, *Journal of Materials Processing Technology*, 201 (1-3) (2008) 574-579.

[15] T. Ghosh et al., A surrogate-assisted optimization approach for multi-response end milling of aluminium alloy AA3105, *The International Journal of Advanced Manufacturing Technology*, 111 (2020) 2419-2439.

[16] V. V. N. Sarath and N. Tamiloli, Optimization of multiple quality characteristics for end milling under dry cutting environment using desirability function, *Journal of Physics: Conference series*, 2070 (2021) 012218.

[17] K. S. Vijaysekar et al., Investigation into the end-milling Parameters of Mg/B_4C metal matrix composites, *Engineering Proceedings,* 61 (1) (2023) 33.

[18] B. C. Kar et al., Research trends in high-speed milling of metal alloys: a short review, *Material Today Proceedings,* 26 (2) (2020) 2657-2662.

[19] G. V. Reddy et al., Tool wear investigation and optimization in milling novel AZ31+SiC MMMC and comparing the results with as authentic AZ31 alloy, *2022 14th International Conference on*

Mathematics, Actuarial Science, Computer Science and Statistics (MACS), Karachi, Pakistan (2022).

R. Venkatesh has obtained a B.E. degree in Mechanical Engineering from the University of Madras, Chennai. He post-graduated in Engineering Design from Anna University, Chennai and obtained his Ph.D. in the faculty of Mechanical Engineering from the College of Engineering Guindy (CEG), Anna University, Chennai. His research interests include nanocomposites, fiber and polymers and solar energy.